

# Modeling immunotherapy and outcomes in acute myeloid leukemia

|       |  |
|-------|--|
| メタデータ | 言語: eng<br>出版者:<br>公開日: 2018-07-03<br>キーワード (Ja):<br>キーワード (En):<br>作成者: 西山, 宣昭<br>メールアドレス:<br>所属: |
| URL   | <a href="https://doi.org/10.24517/00051446">https://doi.org/10.24517/00051446</a>                  |

This work is licensed under a Creative Commons Attribution-NonCommercial-ShareAlike 3.0 International License.



# Modeling immunotherapy and outcomes in acute myeloid leukemia

Yoshiaki NISHIYAMA<sup>1</sup> and Nobuaki NISHIYAMA<sup>1,2,\*</sup>

<sup>1</sup>Graduate School of Natural Science and Technology, Kanazawa University,

<sup>2</sup>Institute of Liberal Arts and Science, Kanazawa University,  
Kanazawa, 920-1192, Japan

(Received November 10, 2017 and accepted in revised form February 1, 2018)

**Abstract** Very recently, we proposed an ordinary differential equation model incorporating promotion of regulatory T cell (Tregs) expansion by leukemic cells, which describes co-evolutional dynamics between leukemic and immune cells in progression of acute myeloid leukemia (AML). To evaluate the ability of our model to predict effectiveness of immunotherapy for AML, we performed Monte Carlo simulation of trajectories in phase plane and generated relapse free survival (RFS) curves, which could be compared with clinical data. The resulting RFS curves were in good accordance with clinical outcomes reported in immunotherapies of NK cells infusion with/without Tregs depletion. In addition, our simulation results focusing on consecutive cycles of cell infusion with/without cell depletion qualitatively accounts for the effectiveness of corresponding clinical immunotherapy. The present results suggest that our model may provide valuable information for future design of immunotherapy in AML.

**Keywords.** acute myeloid leukemia; computational model; regulatory T cells; bistability; relapse free survival curve

## 1 Introduction

Although the vast majority of patients with newly diagnosed acute myeloid leukemia (AML) achieve cytological complete remission (CR) with induction chemotherapy, they have poor prognosis with an overall 5-year survival rate of approximately 27 % due to relapse, despite following consolidation therapy. While cell survival leading to AML relapse is associated with clonal heterogeneity already existing at diagnosis [1], there is accumulating evidence that immunosuppressive AML microenvironments developing through interaction of immune cells with leukemic cells contribute to disease progression and relapse.

AML antigen-specific cytotoxic T lymphocytes (CTLs) are detected in both peripheral blood and bone marrow of patients and have the capacity to kill leukemic cells. Conversely, over expression of immunosuppressive molecules in leukemic cells leads to CTL inhibition, proliferation of leukemic cells and leukemia progression through multiple mechanisms. Regulatory T cells (Tregs) defined by transcription factor FoxP3 expression play a key role in such immunosuppressive mechanisms. While Tregs physiologically play critical roles in the immune tolerance to suppress

---

\*Corresponding author E-mail: nnishiya@staff.kanazawa-u.ac.jp

excessive responses in allergy or autoimmunity[2,3], Tregs have an increased frequency in patients with AML[4] and suppress the effector T cells (Teffs) including natural killer (NK) cells and CTLs. The expressions of PD-L1, a ligand for programmed death-1 (PD-1) receptor, indoleamine 2,3-dioxygenase (IDO) and CD200, a type-1 transmembrane glycoprotein in leukemic cells promote formation of Tregs[5-8]. An increased frequency of Tregs induced by such immunosuppressive molecules results in CTLs suppression and immune evasion.

Allogeneic hematopoietic stem cell transplantation (alloHSCT) as post-remission therapy is still a promising treatment option to prevent relapsing leukemia, in which donor T cells is expected to eliminate residual leukemia cells. While the curative efficacy of HSCT logically has led to the infusion of manipulated T cells to have enhanced anti-leukemic cytotoxic ability, or the activation of endogenous T cells by supportive cytokine therapy for patients without suitable donors, there has been considerable interest in targeting Tregs mediated-suppression of anti-AML reactive T cells. In a rodent model with advanced AML, the efficacy of adoptive CTL therapy was improved by preceding depletion of endogenous Tregs using IL-2 diphtheria toxin (IL-2DT) [9]. Tregs depletion by IL-2DT improves CR rates and disease-free survival of patients with relapsed or refractory AML receiving NK cells infusion[10]. A phase 1 study of Tregs-depleted donor lymphocyte infusion for patients with relapsed AML showed promising results of improved outcomes[11].

Our aim is to construct a mechanistic mathematical model for leukemia dynamics under the impact of developing immunosuppressive environment, which contributes to design protocols of immunotherapy for leukemia. Very recently, we proposed an ordinary differential equation model to describe the dynamics of three components in AML: leukemic blast cells (L), matured Tregs (Treg) and matured effective T cells (Teff) including NK cells and CTLs, in which L promotes Treg expansion[12]. Several mathematical modeling have focused on the interaction of immune cells with leukemic cells[13-15]. These models incorporated the leukemic cell expansion, the promotion of cytotoxic immune cell expansion by leukemic cells (immunogenicity), the killing of leukemic cells by cytotoxic immune cells, and offered explanations for leukemia dynamics observed with and without chemotherapy. In modeling of the impact of tyrosine kinase targeting on chronic myelogenous leukemia (CML) dynamics in patients, immunosuppression was formulated by the decrease of anti-leukemia T cell expansion rate with increasing leukemic cell concentration[16,17]. Recently, in modeling tumor responses and outcomes under immunotherapy combined with radiotherapy, targeting of PD-1, PD-L1 or cytotoxic T-lymphocyte associated protein 4 (CTLA-4) as immunosuppressive mechanism in cancer progression was distinctly incorporated[18]. Our mathematical model incorporates leukemic cell-dependent expansion of immunosuppressive Tregs, which none of these models have considered as a potential target of cancer immunotherapy.

Some modeling interactions between cancer and immune cells allowed multiple steady states and focused on the effectiveness of transitions between the basins of attraction by hypothetical radiation therapy and/or chemotherapy [19-21]. While cell-cell interactions including immunosuppressive mechanism in our model also give rise to two stable steady states corresponding to high and low concentrations of leukemic cell (L), our preliminary result was that longer CR durations observed in AML could be interpreted as transient dynamics in which the system spends longer time in the neighborhood of basin boundary before returning to the steady state with high concentration of L [12]. In the present study, the distribution of CR durations simulated by our model is translated to relapse free survival (RFS) curve which could be compared with clinical outcomes in immunotherapy of AML, resulting in the validation of the ability to predict the impact of immunotherapy such as Tregs targeting and to design immunotherapy protocols for AML.

## 2 Material and Methods

The temporal evolution of the model schematized in Fig.1 is governed by a set of 3 kinetic equations as follows [12].

$$\begin{aligned}
 \frac{d[L]}{dt} &= a_L \left( \frac{k_1^p}{k_1^p + [T_{eff}]^p} \right) - d_L [L] \\
 \frac{d[T_{eff}]}{dt} &= a_{T_{eff}} \left( \frac{k_2^p}{k_2^p + [T_{reg}]^p} \right) - d_{T_{eff}} [T_{eff}] \\
 \frac{d[T_{reg}]}{dt} &= a_{T_{reg}} \left( \frac{[L]^p}{k_3^p + [L]^p} \right) - d_{T_{reg}} [T_{reg}]
 \end{aligned} \tag{1}$$

We consider the populations of leukemic blast cells (L), mature regulatory T cells (Treg), and mature effective T cells (Teff), including CTLs and NK cells. We assume that the dynamics of each cell population (L, Treg, Teff) are due to constant influx and first order decay by apoptosis, in which constant influx rates are denoted by  $a_L$ ,  $a_{Treg}$ ,  $a_{Teff}$ , and decay rate constants are denoted by  $d_L$ ,  $d_{Treg}$ ,  $d_{Teff}$ . Three intercellular interactions were modeled as Hill functions with threshold constants ( $k_1$ ,  $k_2$ ,  $k_3$ ) specifying the strength of intercellular interactions and the Hill coefficient  $p$  [12].

We assume that the concentrations of drugs are constant and the decay rate of each cell population (L, Treg, Teff) is proportional only to the cell population ([L], [Treg], [Teff]) during hypothetical chemotherapy. The rate constants of decay due to apoptosis and drugs are accordingly combined together as  $d_L$ ,  $d_{Treg}$ ,  $d_{Teff}$  during the chemotherapy. Toffs infusion and Tregs depletion as hypothetical immunotherapy were modeled by instantaneous increases and decreases in [Teff] and [Treg], respectively.

Some parameters ( $a_{Treg}$ ,  $a_{Teff}$ ,  $d_{Treg}$ ,  $d_{Teff}$ ) in Eq. (1) were estimated using Bayesian inference via a Markov chain Monte Carlo (MCMC) technique (SAS v.9.4 (SAS Institute, Cary, NC)) with clinical data [22] of lymphocytes recovery after induction chemotherapy [12]. While keeping the parameters  $a_{Treg}$ ,  $a_{Teff}$ ,  $d_{Treg}$  and  $d_{Teff}$  to estimated values by the MCMC method, we searched a wide range of the parameter space of  $a_L$ ,  $d_L$ ,  $k_1$  and found parameter ranges characterized by the existence of one or two stable steady states separated by an unstable fixed point [12]. The values of  $k_2$ ,  $k_3$  and  $p$  were fixed to be those in parameter ranges of bistability. However, we cannot exclude the existence of different dynamics, such as a limit cycle. The values of model parameters in the present study are listed in Table 1.

Steady states of the model were determined as the intersection of three nullclines ( $d[L]/dt = 0$ ,  $d[Teff]/dt = 0$  and  $d[Treg]/dt = 0$ ), which were numerically solved using the `nleqslv` R-package [23]. The ordinary differential equations in Eq.(1) were numerically solved by `ode23` using second and third order Runge-Kutta-Fehlberg formulas with automatic step-size from MATLAB (Ver. 7.13; The Mathworks, Inc.).

## 3 Results

Very recently, we showed that our proposed model offers bistable steady states (denoted as SShi and SSlo) with low and high concentration of leukemic blast cell (L), which could be respectively interpreted as long-term CR and relapsed disease state [12]. The locations of two stable steady states in three dimensional space defined by the concentrations of L, Teff and Treg are  $[L]=100000/\mu\text{L}$ ,  $[Teff]=0.00031/\mu\text{L}$ ,  $[Treg]=4955/\mu\text{L}$  for SShi and  $[L]=40/\mu\text{L}$ ,  $[Teff]=283/\mu\text{L}$ ,  $[Treg]=8/\mu\text{L}$  for SSlo.

We assume that [L] is approximately to be a constant [L]<sub>ss</sub> during complete remission (CR) after

intensive induction chemotherapy. While  $< 5\%$  as the percentage of leukemic blast cells present within the total of nucleated cells in bone marrow is given as a clinical criteria for CR in AML, there is no definitive criteria of peripheral circulating blasts count during CR. According to the clinical observation that 0% to 5% peripheral blast cells during CR had no effects on relapse free survival (RFS) time[24], we could set  $500/\mu\text{L}$  as  $[L]_{ss}$  during CR with 5% peripheral blast cells and  $10000/\mu\text{L}$  as normal counts of peripheral nucleated cells. Together, we had the definition of CR duration as the time interval with less than  $500/\mu\text{L}$  of  $[L]$ . In addition, our interpretation of SSlo as long-term CR was rationalized by the definition of CR duration as  $[L]=40/\mu\text{L}$  of SSlo is less than the threshold  $[L]=500/\mu\text{L}$ . SShi of  $[L]=100000/\mu\text{L}$  is also consistent with cell counts of peripheral leukemic blast in relapsed patients with AML[25].

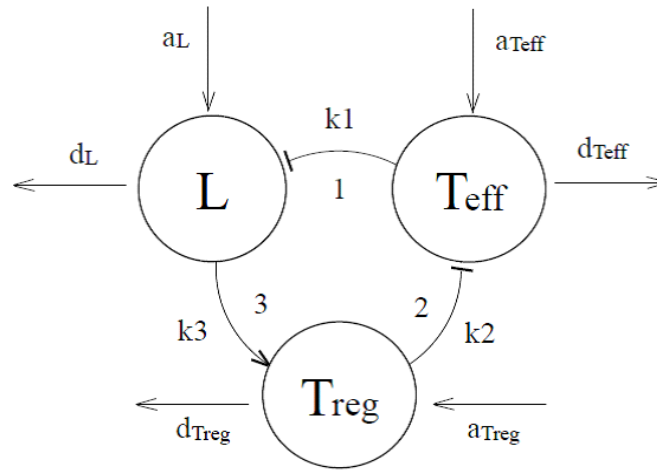


Figure 1. Mechanistic model for crosstalk among leukemic cells and immune cells in AML. The processes of cell-cell interaction are numbered as follows: 1. Leukemic blast cells targeted by effector T cells, 2. Effector T cell suppression mediated by Treg, and 3. Treg formation promoted by leukemic blast cells (L).

Table 1: Parameter values used in the simulation

| Symbol            | Value  |
|-------------------|--|
| cell influx       |  |
| $a_L$             | $0.1 - 1000 \mu\text{L}^{-1}\text{day}^{-1}$ |
| $a_{\text{Teff}}$ | $56.53 \mu\text{L}^{-1}\text{day}^{-1}$      |
| $a_{\text{Treg}}$ | $198.2 \mu\text{L}^{-1}\text{day}^{-1}$      |
| cell decay        |  |
| $d_L$             | $0.0001 - 1.0 \text{ day}^{-1}$              |
| $d_{\text{Teff}}$ | $0.2 \text{ day}^{-1}$                       |
| $d_{\text{Treg}}$ | $0.04 \text{ day}^{-1}$                      |
| cell interaction  |  |
| $k_1$             | $1 - 1000 \mu\text{L}^{-1}$                  |
| $k_2$             | $160 \mu\text{L}^{-1}$                       |
| $k_3$             | $200 \mu\text{L}^{-1}$                       |
| hill coefficient  |  |
| $p$               | $1 - 10$                                     |

Fig.2 shows time-courses of concentrations of L, Teff and Treg in the case of hypothetical chemotherapy applied to the stable steady state (SShi) with high L load. With the definition of CR duration, it is found in Fig.2 that the system returns to the original steady state (SShi) with transient increase of Teff concentration during CR. CR duration depends on the arrived location in the phase plane of [L], [Teff] and [Treg] by hypothetical chemotherapies[12]. It also depends on the arrived location whether the system is forced to go to SSlo or return to SShi[12].

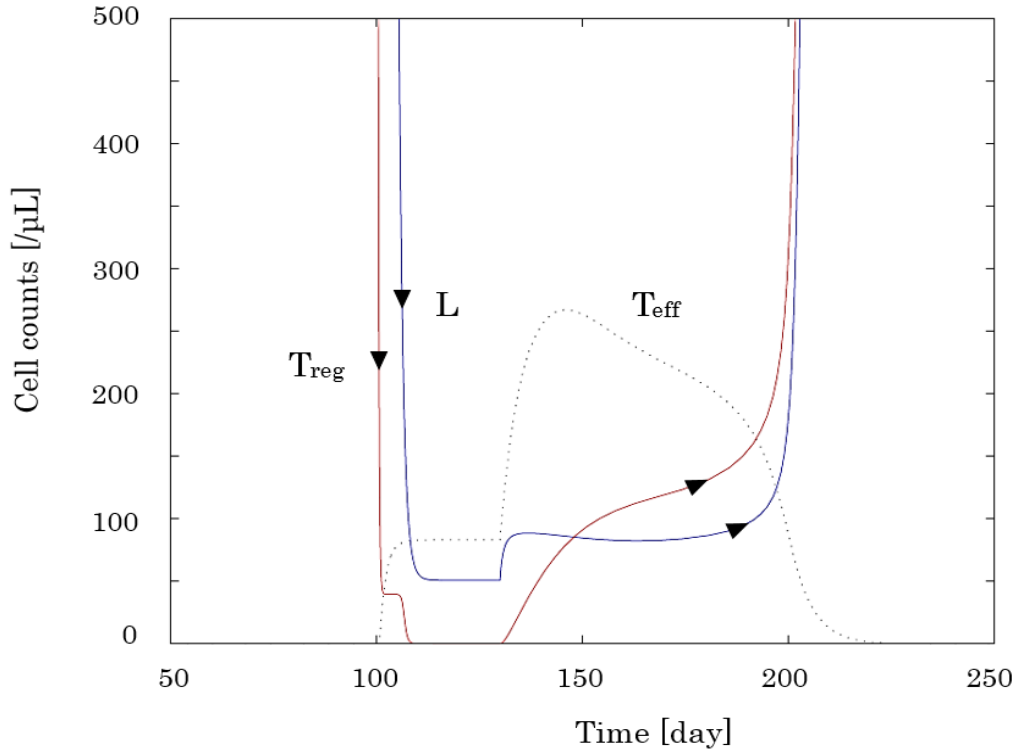


Figure 2. Time courses of [L], [Teff] and [Treg] after chemotherapy applied for the system staying at SShi. Solid lines are for [L] (blue) and [Treg] (red) and dots are for [Teff]. Parameter values are  $a_L=1000$ ,  $a_{Teff}=56.53$ ,  $a_{Treg}=198.2$ ,  $d_L=0.01$ ,  $d_{Teff}=0.2$ ,  $d_{Treg}=0.04$ ,  $k_1=40$ ,  $k_2=160$ ,  $k_3=200$ ,  $p=4$ . The chemotherapy was applied with enhanced cell decay rate constants ( $d_L=1.0$ ,  $d_{Teff}=0.68$ ,  $d_{Treg}=5.0$ ) during 30 days. The system goes towards the original SShi after the chemotherapy with transient increase of [Teff].

We performed Monte Carlo simulation of the trajectories from the stable steady state (SShi) with high L load after hypothetical chemotherapy applied with random sampling from normal distributions of three rate constants of cell decay ( $d_L$ ,  $d_{Teff}$ ,  $d_{Treg}$ ). The distributions of resulting CR durations were translated into relapse free survival (RFS) curves as shown in Fig.3. Fig.3 shows one example of RFS curves in the cases of instantaneous Teffs infusion with/without preceding Tregs depletion. This result suggests that infusion of Teffs such as NK cells and CTLs accompanying with conventional chemotherapy is effective for outcome improvement. The assumption of normal distributions for the rate constants was originated from patient-to-patient variability of sensitivity for chemotherapy. The effectiveness of Teffs infusion with/without preceding Tregs depletion was confirmed with normal distributions for  $d_L$ ,  $d_{Teff}$ ,  $d_{Treg}$  with a wide range of standard deviations. In Fig.3, it is found that the three curves converge to steady ratios of RFS, which correspond to the ratios of the trajectories from SShi to SSlo without relapse, compared with the trajectories returning to the original steady state SShi. We repeated 10 times of generating RFS curves corresponding to

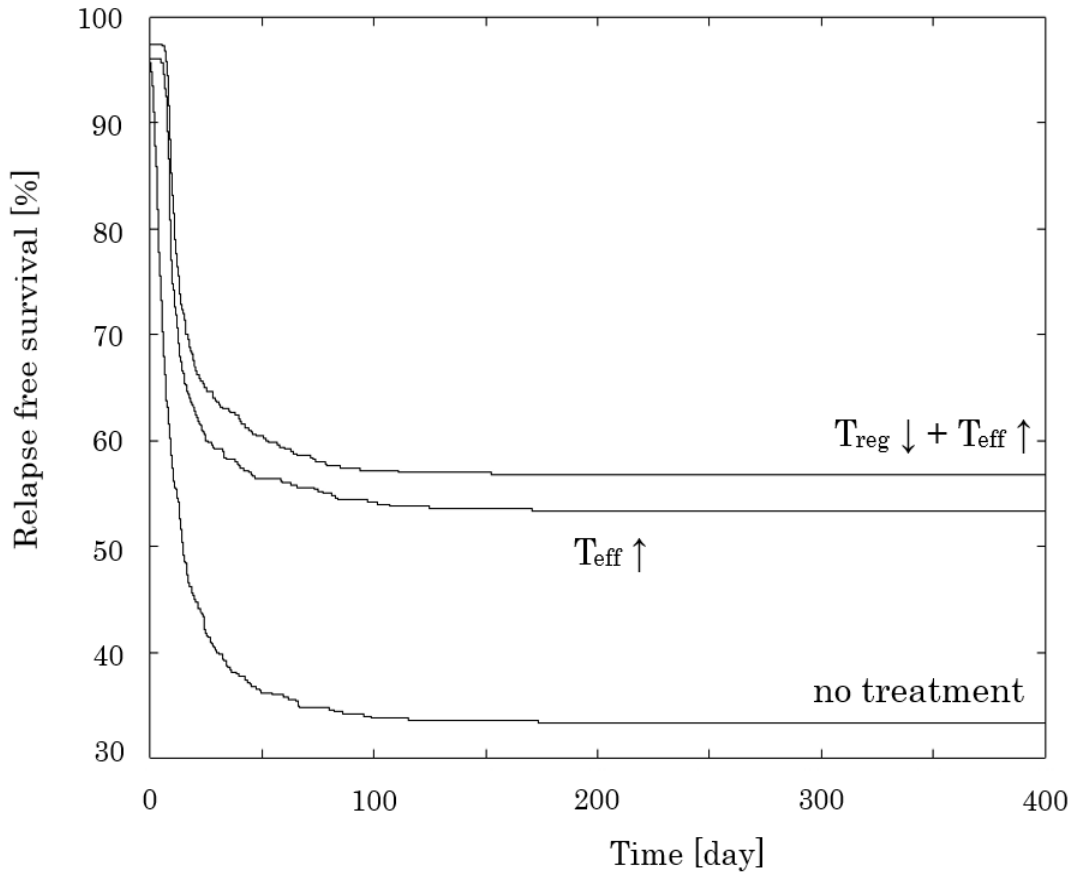


Figure 3. Relapse free survival (RFS) curves in the cases of Teffs infusion with/without Tregs depletion and no treatment after chemotherapy. The relapse was defined as the event that the system overrides the threshold of  $[L]$  towards SS<sub>hi</sub> from CR states, and the duration of CR as a time interval from the termination of chemotherapy to the crossing of the threshold. The threshold was set to be  $[L]=500/\mu\text{L}$ . 500 trajectories from SS<sub>hi</sub> by applying chemotherapy during 30 days were calculated with  $d_L$ ,  $d_{Teff}$ ,  $d_{Treg}$  of the values selected randomly from normal distributions of  $N(1.0,0.33)$ ,  $N(0.75,0.25)$ ,  $N(5.0,1.67)$ , respectively. Instantaneous Teffs infusion or Tregs depletion was applied after 0.0001 days from time point of chemotherapy termination. The instantaneous Tregs depletion was followed by instantaneous Teffs infusion with a time interval of 0.0002 days. Increment of  $[Teff]$  by instantaneous infusion was set to be  $200/\mu\text{L}$  and decrement of  $[Treg]$  by instantaneous depletion was set to be  $100/\mu\text{L}$ . Parameter values are  $a_L=1000$ ,  $a_{Teff}=56.53$ ,  $a_{Treg}=198.2$ ,  $d_L=0.01$ ,  $d_{Teff}=0.2$ ,  $d_{Treg}=0.04$ ,  $k_1=40$ ,  $k_2=160$ ,  $k_3=200$ ,  $p=4$ . The number of the trajectories without occurring relapse was plotted against the CR duration of the last trajectory with relapse.

those shown in Fig.3. The resulting RFS ratios at 700 days after the termination of chemotherapy were  $35.6\pm 2.2\%$ ,  $54.8\pm 2.7\%$  and  $54.8\pm 2.6\%$  for no treatment, Teffs infusion, and Teffs infusion with preceding Tregs depletion, respectively. Fig.4 shows the impacts of hypothetical chemotherapy only and Teffs infusion with preceding Tregs depletion after chemotherapy with random sampling from normal distributions of three cell decay rates. The incoming trajectories from SS<sub>hi</sub> are divided into those converging to SS<sub>hi</sub> and to SS<sub>lo</sub>. More trajectories converging to SS<sub>lo</sub> in the case of Teffs infusion with preceding Tregs depletion are observed, which are compared with the case of chemotherapy only and are consistent with higher ratios of RFS in the cases of Teffs infusion with/without preceding Tregs depletion, as shown in Fig.3. In our modeling, the effect of treatments of chemotherapy combined with/without Teffs infusion with/without preceding Tregs depletion depends on whether the system overrides the basin boundary and is forced to enter the basin of

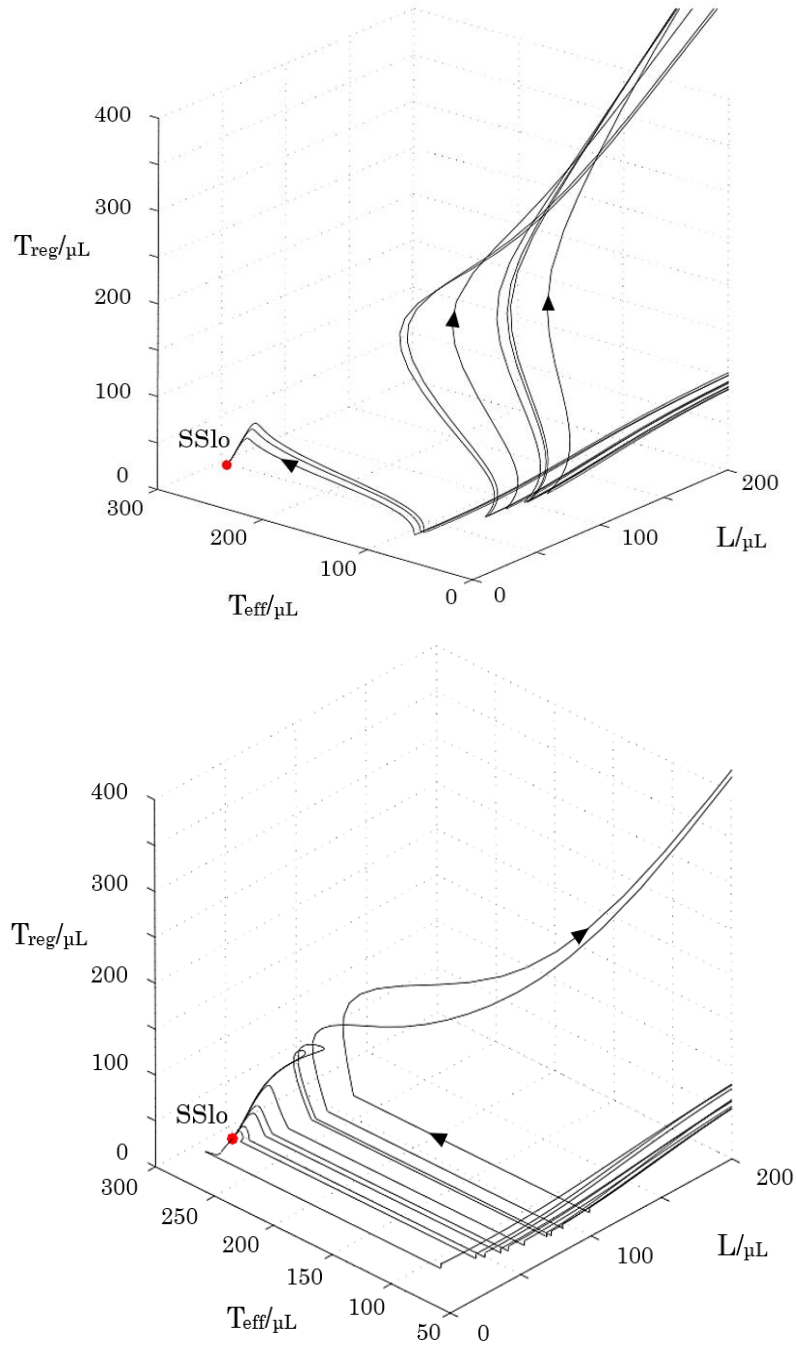


Figure 4. 10 trajectories from SS<sub>hi</sub> (out of figure) by applying chemotherapy only (upper figure) and chemotherapy followed by instantaneous Teffs infusion with preceding Tregs depletion (lower figure). 10 trajectories from SS<sub>hi</sub> by applying chemotherapy during 30 days were calculated with  $d_L$ ,  $d_{Teff}$ ,  $d_{Treg}$  of the values selected randomly from normal distributions of  $N(1.0, 0.33)$ ,  $N(0.75, 0.25)$ ,  $N(5.0, 1.67)$ , respectively. Instantaneous Tregs depletion was applied after 0.0001 days from time point of chemotherapy termination. The instantaneous Tregs depletion was followed by instantaneous Teffs infusion with time interval of 0.0002 days. Increment of  $[T_{eff}]$  by instantaneous infusion was set to be  $200/\mu\text{L}$  and decrement of  $[T_{reg}]$  by instantaneous depletion was set to be  $5/\mu\text{L}$ . Parameter values are  $a_L=1000$ ,  $a_{Teff}=56.53$ ,  $a_{Treg}=198.2$ ,  $d_L=0.01$ ,  $d_{Teff}=0.2$ ,  $d_{Treg}=0.04$ ,  $k_I=40$ ,  $k_2=160$ ,  $k_3=200$ ,  $p=4$ .

attraction of SSlo from one of SS<sub>hi</sub>. The basin boundary is shown in Fig.5, in which one trajectory from SS<sub>hi</sub> intersects the basin boundary and converges to SSlo, while another trajectory stays in the basin of attraction of SS<sub>hi</sub> and returns to SS<sub>hi</sub>. The existence of the basin boundary suggests that infusion of higher number of Teff cells could be associated with treatment efficiency. While the impact of infused cell number may be crucial for treatments of cell transplantation, some works has been devoted to clarify the role of multiple cell infusions, which could avoid graft-versus-host disease (GVHD) with reduced number of infused cells [26]. As our modeling directs to future design of protocols of combined immunotherapy with chemotherapy in AML, the effectiveness of consecutive cycles of instantaneous Teffs infusion with/without preceding Tregs depletion as hypothetical immunotherapies was examined. Fig.6 shows time schedule of induction chemotherapy followed by consecutive cycles of instantaneous Teffs infusion with preceding Tregs depletion. The first Tregs depletion was applied with a time interval (duration 0) after induction chemotherapy. Time intervals between Tregs depletion and Teffs infusion were set to be constant (duration 1). Time intervals between two Teffs infusions in the case of Teffs infusion without Tregs depletion were double time of duration 1. Fig.7 shows one example of RFS curves for 5 cycles of Teffs infusion without Treg depletion and Teffs infusion with preceding Tregs depletion, compared with the case of no treatments. Fig.8 shows dependence of relapse free survival (RFS) rate on the number of consecutive cycles of instantaneous Teffs infusion with/without preceding Tregs depletion, compared with the case of no treatment. We repeated 10 times of generating RFS curves corresponding to those shown in Fig.7. The resulting RFS ratios at 700 days after the termination of chemotherapy were  $36.5 \pm 2.7\%$ ,  $54.1 \pm 1.8\%$  and  $56.7 \pm 2.1\%$  respectively for no treatment, 5 cycles of Teffs infusion, and 5 cycles of Teffs infusion with preceding Tregs depletion, as shown in Fig.8. It should be noted that increment of [Teff] by each instantaneous infusion was set to be  $40/\mu\text{L}$  and decrement of [Treg] by each instantaneous depletion was set to be  $20/\mu\text{L}$  in Fig.7 and 8, compared with increment of [Teff] ( $200/\mu\text{L}$ ) and decrement of [Treg] ( $100/\mu\text{L}$ ) in the case of Fig.3. Fig.9 shows examples in the cases of 3 cycles and 5 cycles of Teffs infusion with preceding Tregs depletion, suggesting effectiveness of more cycles of the treatment. These results shown in Fig.7, 8 and 9 suggest the effectiveness of consecutive cycles of immunotherapy with less doses of Teffs infusion and Tregs depletion.

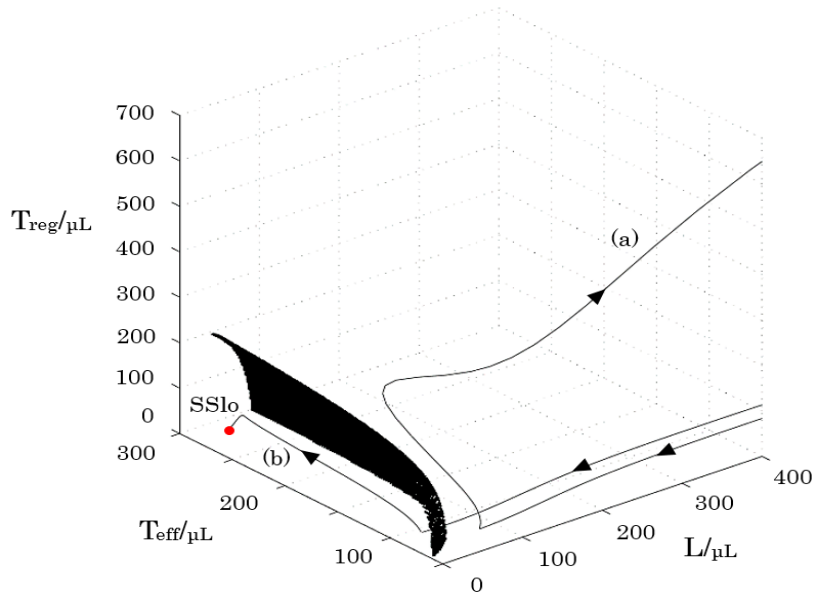


Figure 5. The basin boundary denoted by a dotted plane and two trajectories from SS<sub>hi</sub> (out of figure). Parameter values are  $a_L=1000$ ,  $a_{Teff}=56.53$ ,  $a_{Treg}=198.2$ ,  $d_L=0.01$ ,  $d_{Teff}=0.2$ ,  $d_{Treg}=0.04$ ,  $k_1=40$ ,  $k_2=160$ ,  $k_3=200$ ,  $p=4$ . Two trajectories from SS<sub>hi</sub> by applying chemotherapy during (a) 10 days and (b) 30 days were calculated with the values of (a)  $d_L=1.0$ ,  $d_{Teff}=0.75$ ,  $d_{Treg}=5.0$  and (b)  $d_L=1.0$ ,  $d_{Teff}=0.6$ ,  $d_{Treg}=5.0$ .

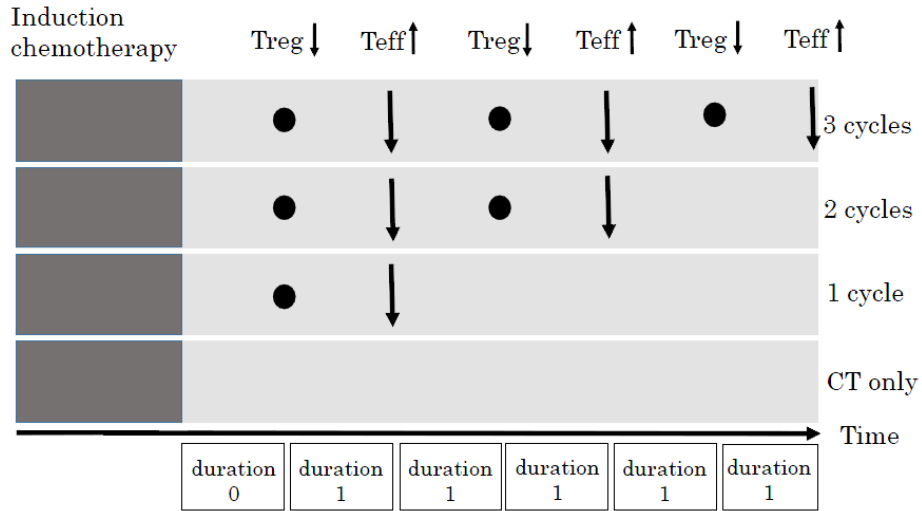


Figure 6. Time schedule of induction chemotherapy followed by consecutive cycles of instantaneous Teffs infusion with preceding Tregs depletion. The first Tregs depletion was applied with a time interval (duration 0) after induction chemotherapy. Time intervals between Tregs depletion and Teffs infusion were set to be constant (duration 1). Arrows denote time points of instantaneous Teffs infusion and closed circles denote time points of instantaneous Tregs depletion.

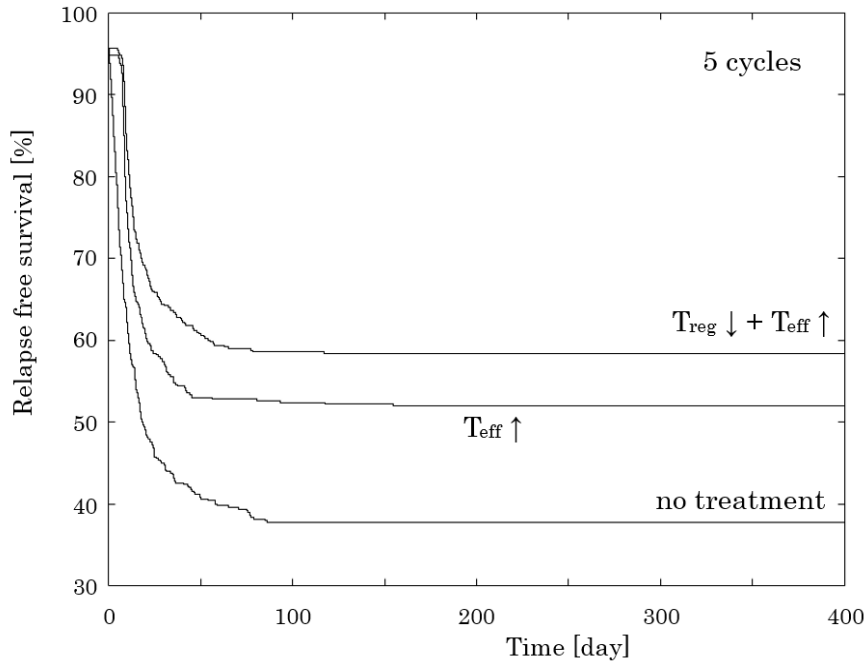


Figure 7. Relapse free survival (RFS) curves in the cases of 5 consecutive cycles of Teff cells infusion with/without Treg cells depletion and no treatment after chemotherapy. The threshold for relapse was set to be  $[L]=500/\mu\text{L}$ . 500 trajectories from SShi by applying chemotherapy during 30 days were calculated with  $d_L, d_{Teff}, d_{Treg}$  of the values selected randomly from normal distributions of  $N(1.0,0.33), N(0.75,0.25), N(5.0,1.67)$ , respectively. Instantaneous Teffs infusion or Tregs depletion was applied after 0.0001 days from time points of chemotherapy termination. The instantaneous Tregs depletion was followed by instantaneous Teffs infusion with time interval of 0.0002 days. Increment of  $[Teff]$  by each instantaneous infusion was set to be  $40/\mu\text{L}$  and decrement of  $[Treg]$  by each instantaneous depletion was set to be  $20/\mu\text{L}$ . Parameter values are  $a_L=1000, a_{Teff}=56.53, a_{Treg}=198.2, d_L=0.01, d_{Teff}=0.2, d_{Treg}=0.04, k_1=40, k_2=160, k_3=200, p=4$ . The number of the trajectories without occurring relapse was plotted against the CR duration of the last trajectory with relapse.

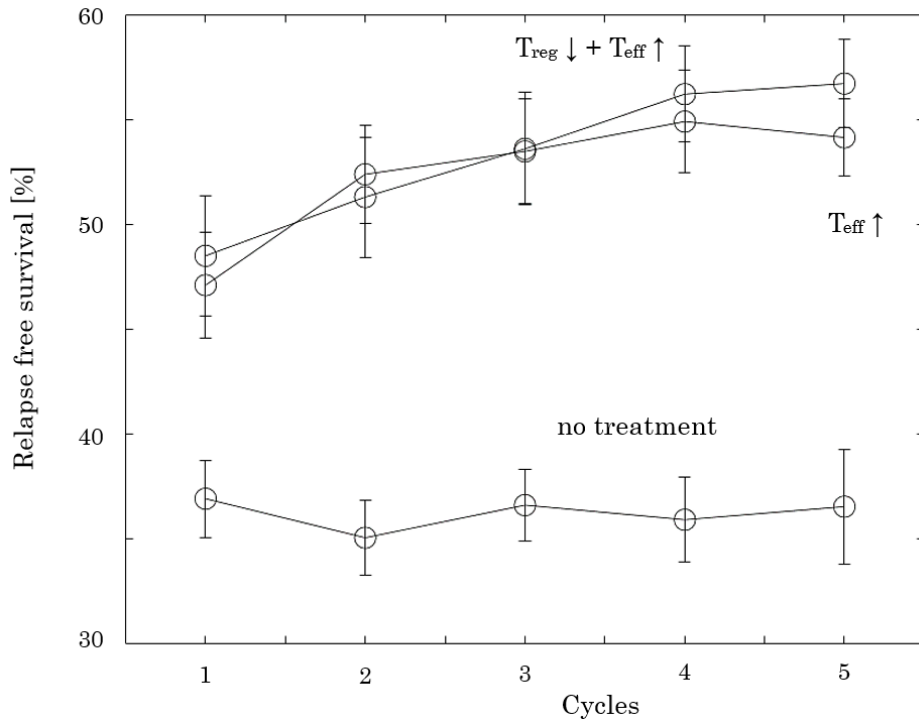


Figure 8. Dependence of relapse free survival (RFS) rate on the number of consecutive cycles of instantaneous Teffs infusion or instantaneous Tregs depletion followed by instantaneous Teffs infusion. The RFS rates after 700 days from the time point of chemotherapy termination are indicated. The RFS rates were based on RFS curves which were estimated from 500 trajectories. Standard deviations in the figure were estimated from 10 RES curves. 500 trajectories from SShigh by applying chemotherapy during 30 days were calculated with  $d_L$ ,  $d_{Teff}$ ,  $d_{Treg}$  of the values selected randomly from normal distributions of  $N(1.0,0.33)$ ,  $N(0.75,0.25)$ ,  $N(5.0,1.67)$ , respectively. Instantaneous Teffs infusion or Tregs depletion was applied after 0.0001 days from the time point of chemotherapy termination. The instantaneous Tregs depletion was followed by instantaneous Teffs infusion with time interval of 0.0002 days. Increment of [Teff] by each instantaneous infusion was set to be  $40/\mu\text{L}$  and decrement of [Treg] by each instantaneous depletion was set to be  $20/\mu\text{L}$ . Parameter values are  $a_L=1000$ ,  $a_{Teff}=56.53$ ,  $a_{Treg}=198.2$ ,  $d_L=0.01$ ,  $d_{Teff}=0.2$ ,  $d_{Treg}=0.04$ ,  $k_1=40$ ,  $k_2=160$ ,  $k_3=200$ ,  $p=4$ .

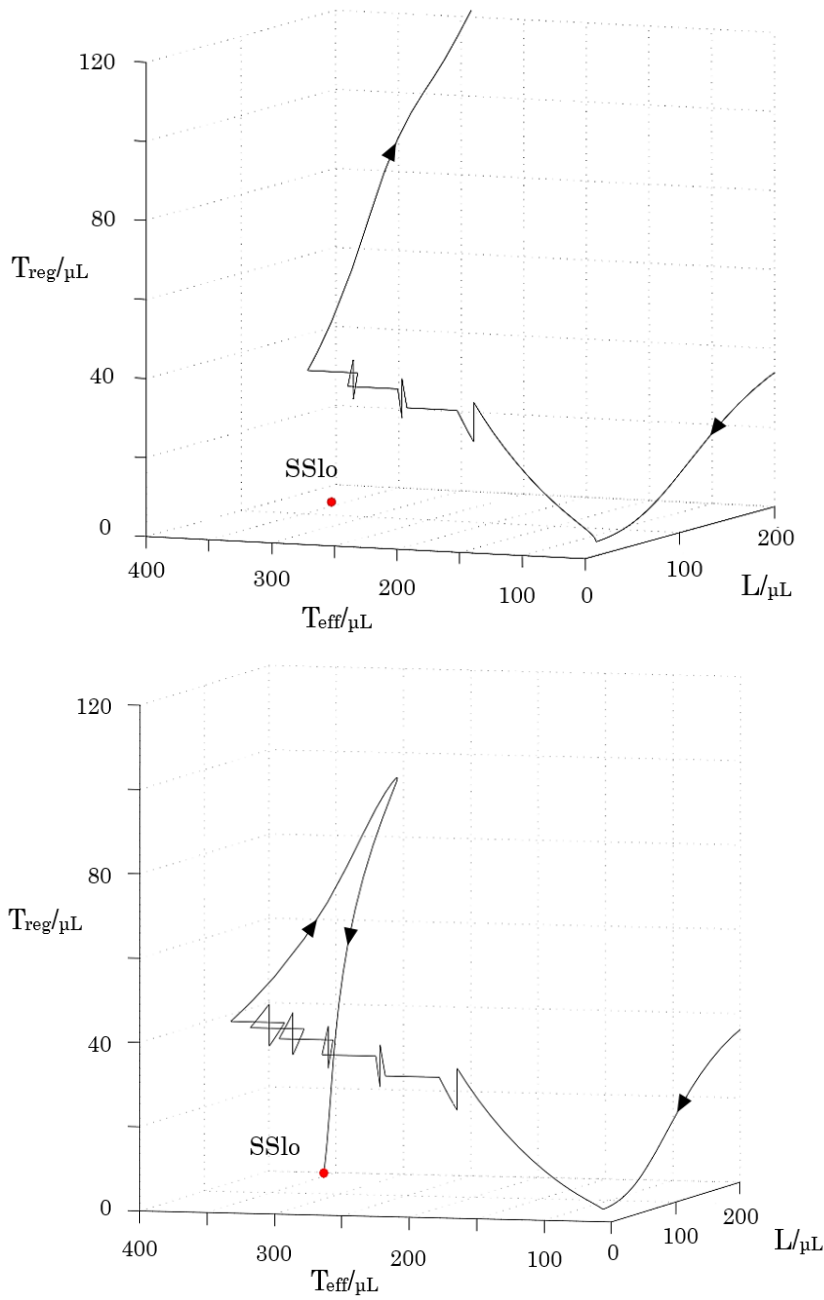


Figure 9. The trajectories from SS<sub>hi</sub> (not shown in figure) after chemotherapy followed by consecutive cycles of instantaneous Teffs infusion with preceding Tregs depletion: (upper figure) 3 cycles, (lower figure) 5 cycles. Parameter values are  $a_L=1000$ ,  $a_{Teff}=56.53$ ,  $a_{Treg}=198.2$ ,  $d_L=0.01$ ,  $d_{Teff}=0.2$ ,  $d_{Treg}=0.04$ ,  $k_1=40$ ,  $k_2=160$ ,  $k_3=200$ ,  $p=4$ . Chemotherapy during 30 days were applied with  $d_L=1.0$ ,  $d_{Teff}=0.69$ ,  $d_{Treg}=5.0$ . First instantaneous Tregs depletion was applied after 0.0001 days from the time point of chemotherapy termination. The instantaneous Tregs depletions were followed by instantaneous Teff infusions with the time interval of 0.0002 days. Increment of [Teff] by each instantaneous infusion was set to be 40/ $\mu$ L and decrement of [Treg] by each instantaneous depletion was set to be 20/ $\mu$ L.

## 4 Discussion

Our model proposed recently was capable of explaining variable CR durations as clinical finding [12]. Especially, long-term CR duration was suggested to associate with transient dynamics in the neighborhood of basin boundary [12]. In the present study, we translated the distributions of simulated CR durations into RFS curves which could be compared with clinical data. Curti et al. [27] suggested the effectiveness of allogeneic NK cell infusion as post CR consolidation treatment for elderly AML patients and identified higher number of infused NK cells as a favorable prognostic factor. They reported improved outcomes for patients in CR receiving NK cells infusion (n=16, RFS ratio=0.56 with a median follow-up of 22.5 months), compared with non-NK cells-treated control (n=15, RFS ratio=0.25). Bachanova et al. focused on the impact of preceding Tregs depletion followed by NK cells infusion, with the hypothesis that Tregs may suppress the effectiveness of anti-leukemic NK cell infusion [10]. Patients with refractory AML received Tregs depletion with IL-2 diphtheria toxin (IL2DT), which could selectively deplete IL-2 receptor expressing cells, including Tregs. They reported that RFS ratio is 33% (n=42) at 6 month after NK cells infusion with adding IL2DT, compared with 5% for patients (n=15) receiving only NK cells infusion [10]. With our present model, RFS curves were produced numerically by assuming that cell decay rate constants of L, Teff and Treg characterizing hypothetical chemotherapy are random variables with normal distributions. Despite such simplifications, the model was qualitatively capable to explain the effectiveness of a single infusion of NK cells compared with only chemotherapy, as shown in Fig.3.

In general, consecutive cycles of cell infusion with minimal cell number have been used in immunotherapy, as a single infusion of high number of Teff cells is often associated with higher incidence of GVHD. Dazzi et al. examined the effectiveness of consecutive cycles of donor lymphocyte infusion with lower cell number for relapsed patients with chronic myeloid leukemia [26]. They suggested that the occurrence of GVHD in patients is significantly inhibited with consecutive cycles of cell infusion, compared with that in the case of a single administration of comparable total cell number, while the difference of remission achievement between the two groups is not significant. In general, the protocols of NK cells infusion for AML are in line with this study, in which a single infusion of NK cells is followed by consecutive cycles of IL2 administration for infused NK cell activation [10,27]. Although there are no clinical studies which could directly evaluate our results of the impact of consecutive cycles of instantaneous Teffs infusion with/without preceding Tregs depletion as shown in Fig.8, the effectiveness of consecutive activation of endogenous T cells and NK cells for AML [28-30] supports the ability of our modeling to predict the outcomes. Brune et al. [28] reported that consecutive administration of IL2 and histamine dihydrochloride (HDC) for patients with AML in CR significantly improved RFS, compared with patients with no treatment, which is comparable with our results shown in Fig.8.

## 5 Conclusion

Our model might be proposed to be a candidate to contribute to make determination of optimal dosing and scheduling of immune cell modulation for AML, while the location of the boundary of basins inherent in our model remain to be identified for each individual patient.

## References

- [1] L.I. Shlush, A. Mitchell, L. Heisler, S. Abelson, S.W. K. Ng, A. Trotman-Grant, J. J. F. Medeiros, A.Rao-Bhatia, I. Jaciw-Zurakowsky, R. Marke, J.L. McLeod, M. Doedens, G. Bader, V. Voisin, C.J. Xu, J.D.

- McPherson, T. J. Hudson, J.C.Y. Wang, M.D. Minden, J.E. Dick, Tracing the origins of relapse in acute myeloid-Leukaemia to stem cells, *Nature* 547(7661) (2017) 104-108.
- [2] S. Lind-Ley, C.M. Dayan, A. Bishop, B.O. Roep, M. Peakman, T.I.M. Tree, Defective suppressor function in CD4(+)CD25(+) T-cells from patients with type 1 diabetes, *Diabetes* 54(1) (2005) 92-99.
- [3] R.J. DiPaolo, C. Brinster, T.S. Davidson, J. Andersson, D. Glass, E.M. Shevach, Autoantigen-specific TGF $\beta$ -induced Foxp3<sup>+</sup> regulatory T cells prevent autoimmunity by inhibiting dendritic cells from activating autoreactive T cells, *J Immunol.* 179(7) (2007) 4685-4693.
- [4] M.J. Szczepanski, M. Szajnik, M. Czystowska, M. Mandapathil, L. Strauss, A. Welsh, K.A. Foon, T.L. Whiteside, M. Boyiadzis, Increased Frequency and Suppression by Regulatory T Cells in Patients with Acute Myelogenous Leukemia, *Clin. Cancer Res.* 2009, 15(10) 3325-3332.
- [5] C. Ustun, J.S. Miller, D.H. Munn, D.J. Weisdorf, B.R. Blazar, Regulatory T cells in acute myelogenous leukemia: is it time for immunomodulation? *Blood* 118(19) (2011) 5084-5095.
- [6] A. Curti, S. Pandolfi, B. Va-Lzasina, M. A-Luigi, A. Isidori, E. Ferri, et al., Modulation of tryptophan catabolism by human leukemic cells results in the conversion of CD25<sup>-</sup> into CD25<sup>+</sup> T regulatory cells, *Blood* 109(7) (2007) 2871-2877.
- [7] L.M. Francisco, V.H. Sa-Linas, K.E. Brown, V.K. Vanguri, G.J. Freeman, V.K. Kuchroo, A.H. Sharpe, PD-L1 regulates the development, maintenance, and function of induced regulatory T cells, *J. Exp. Med.* 206(13) (2009) 3015-3029.
- [8] S.J. Coles, R.K. Hills, E.C. Wang, A.K. Burnett, S. Man, R.L. Darley, A. Tonks, Increased CD200 expression in acute myeloid-Leukemia is linked with an increased frequency of FoxP3<sup>+</sup> regulatory T cells, *Leukemia* 26(9) (2012) 2146-2148.
- [9] Q. Zhou, C. Bucher, M.E. Munger, S.L. Highfill, J. Tolar, D.H. Munn, B.L. Levine, M. Ridd-Le, C.H. June, D.A. Vallera, B.J. Weigel, B.R. Blazar, Depletion of endogenous tumor-associated regulatory T cells improves the efficacy of adoptive cytotoxic T-cell immunotherapy in murine acute myeloid-Leukemia, *Blood* 114 (2009) 3793-3802.
- [10] V. Bachanova, S. Cooley, T.E. Defor, M.R. Verneris, B. Zhang, D.H. McKenna, J. Curtsinger, A. Panoskaltsis-Mortari, D-Lewis, K. Hippen, P. McGlave, D.J. Weisdorf, B.R. Blazar, J.S. Miller, Clearance of acute myeloid-Leukemia by haploidentical natural killer cells is improved using IL-2 diphtheria toxin fusion protein, *Blood* 123(25) (2014) 3855-3863.
- [11] S. Nikiforow, H.T. Kim, H. Da-Ley, Carol Reynolds, K.T. Jones, P. Armand, V.T. Ho, E.P.A-Lyea III, C.S. Cutler, J. Ritz, J.H. Antin, R.J. Soiffer, J. Koreth, A phase I study of CD25/regulatory T-cell-depleted donor lymphocyte infusion for relapse after allogeneic stem cell transplantation, *Haematologica* 101(10) (2016) 1251-1259.
- [12] Y. Nishiyama, Y. Saikawa, N. Nishiyama, Interaction between the immune system and acute myeloid leukemia: A model incorporating promotion of regulatory T cell expansion by leukemic cells, *BioSystems* 165(2018)99-105.
- [13] V.A. Kuznetsov, I.A. Makalkin, M.A. Taylor, A.S. Perelson, Nonlinear dynamics of immunogenic tumors: parameter estimation and global bifurcation analysis, *Bull. Math. Biol.* 56(2) (1994) 295-321.
- [14] K. Roesch, D. Hasenclever, M. Scholz, Modelling lymphoma therapy and outcome, *Bull. Math. Biol.* 76(2) (2014) 401-430.
- [15] H. Moore and N.K. Li, A mathematical model for chronic myelogenous (CML) and T cell interaction, *J. theor. Biol.* 227 (2004) 513-523.
- [16] P.S. Kim, P.P. Lee, D-Levy, Dynamics and potential impact of the immune response to chronic myelogenous leukemia, *PLoS Computational Biol.* 4(6) (2008)e1000095.
- [17] G. D. Clapp, T. Lepoutre, R.E. Cheikh, S. Bernard, J. Ruby, H. Labussière-Wallet, F.E. Nicolini, D-Levy, Implication of the Autologous Immune System in BCR-ABL Transcript Variations in Chronic Myelogenous Leukemia Patients Treated with Imatinib, *Cancer Res.* 75(19) (2015) 4053-4062.
- [18] R. Serre, S. Benzekry, L. Padovani, C. Meille, N. André, J. Ciccolini, F. Barlesi, X. Muracciole, D. Barbolosi, Mathematical Modeling of Cancer Immunotherapy and Its Synergy with Radiotherapy, *Cancer Res.* 76(17) (2016) 4931-4940.
- [19] L.G. de Pillis, W. Gu, A.E. Radunskaya, Mixed immunotherapy and chemotherapy of tumors: modeling, applications and biological interpretations, *Journal of theoretical Biology* 238 (2006) 841-862.
- [20] L.G. De Pillis, A. Radunskaya, A mathematical tumor model with immune resistance and drug therapy: an optimal control approach, *Journal of Theoretical Medicine*, 3 (2001) 841-862.
- [21] M. Lu, B. Huang, S.M. Hanash, J.N. Onuchica, E. Ben-Jacob, Modeling putative therapeutic implications of exosome exchange between tumor and immune cells, *Proc. Natl. Acad. Sci. USA*, 111(2014) E4165-E4174.
- [22] C.G. Kanakry, A.D. Hess, C.D. Gocke, C. Thoburn, F. Kos, C. Meyer, et al., Early lymphocyte recovery

- after intensive timed sequential chemotherapy for acute myelogenous leukemia: peripheral oligoclonal expansion of regulatory T cells, *Blood* 117(2) (2011) 608-617.
- [23] B. Hasselman, nleqslv: Solving systems of nonlinear equations, R package version 2.1.1 (2014).
- [24] E.H. Estey, P.F. Thall, X. Wang, S. Verstovsek, J. Cortes, H.M. Kantarjian, Effect of circulating blasts at time of complete remission on subsequent relapse-free survival time in newly diagnosed AML, *Blood* 102 (2003) 3097-3099.
- [25] D. Verma, H. Kantarjian, S. Faderi, S. O'Brien, S. Pierce, K. Vu, E. Freireich, M. Keating, J. Cortes, F. Ravandi, Late relapses in acute myeloid leukemia: analysis of characteristics and outcome, *Leuk. Lymphoma* 51(5) (2010) 778-782.
- [26] F. Dazzi, R.M. Szydlo, C. Craddock, N.C.P. Cross, J. Kaeda, A. Chase, E. Olavarria, F. van Rhee, E. Kanfer, J.F. Apperley, J.M. Goldman, Comparison of single-dose and escalating-dose regimens of donor lymphocyte infusion for relapse after allografting for chronic myeloid-Leukemia, *Blood* 95 (2000) 67-71.
- [27] A. Curti, L. Ruggeri, S. Parisi, A. Bontadini, E. Dan, M.R. Motta, S. Rizzi, S. Trabanelli, D. Ocak-Likova, M. Lecciso, V. Giudice, F. Fruet, E. Urbani, C. Papayannidis, G. Martinelli, G. Bandini, F. Bonifazi, R.E. Lewis, M. Cavo, A. Velardi, R.M. Lemoli, Larger size of donor alloreactive NK cell repertoire correlates with better response to NK cell immunotherapy in elderly acute myeloid-Leukemia patients, *Clin Cancer Res* 22(8) (2016) 1914-1921.
- [28] M. Brune, S. Castaigne, J. Catalano, K. Gehlsen, A.D. Ho, W. Hofmann, D.E. Hogge, B. Nilsson, R. Or, A.I. Romero, J.M. Rowe, B. Simonsson, R. Spearing, E.A. Stadtmauer, J. Szer, E. Wallhult, K. Hellstrand, Improved Leukemia-free survival after postconsolidation immunotherapy with histamine dihydrochloride and interleukin-2 in acute myeloid-Leukemia: results of a randomized phase 3 trial, *Blood* 108 (2006) 88-96.
- [29] A. Hallner, J. Aurelius, F.B. Thoren, F.E. Sander, M. Brune, K. Hellstrand, A. Martner, Immunotherapy with histamine dihydrochloride and Low-dose interleukin-2 favors sustained-Lymphocyte recovery in acute myeloid-Leukemia, *European J. Haematol.* 94 (2014) 279-280.
- [30] F.E. Sander, A. Rydström, E. Bernson, R. Kiffi, R. Riise, J. Aurelius, H. Anderson, M. Brune, R. Foà, K. Hellstrand, F.B. Thorén, A. Martner, Dynamics of cytotoxic T cell subsets during immunotherapy predicts outcome in acute myeloid-Leukemia, *Oncotarget* 7 (2016) 7586-7596.